Timing Acquisition Performance Metrics of Tc-DTR UWB Receivers over Frequency-Selective Fading Channels with Narrow-Band Interference: Performance Analysis and Optimization

Marco Di Renzo, Dario de Leonardis, Fabio Graziosi, Fortunato Santucci

Timing Acquisition Performance Metrics of $\mathrm{T_c}$–DTR UWB Receivers over Frequency–Selective Fading Channels with Narrow–Band Interference

Marco Di Renzo[(1)], Dario De Leonardis[(2)], Fabio Graziosi[(2)], Fortunato Santucci[(2)]
[(1)] L2S, UMR 8506 CNRS – SUPELEC – Univ Paris–Sud
Laboratory of Signals and Systems (L2S), French National Center for Scientific Research (CNRS)
École Supérieure d'Électricité (SUPÉLEC), University of Paris–Sud XI (UPS)
3 rue Joliot–Curie, 91192 Gif–sur–Yvette (Paris), France
[(2)] University of L'Aquila, College of Engineering
Department of Electrical and Information Engineering (DIEI), Center of Excellence for Research DEWS
Via G. Gronchi 18, Nucleo Industriale di Pile, 67100 L'Aquila, Italy
E–Mail: marco.direnzo@lss.supelec.fr, {fabio.graziosi, fortunato.santucci}@univaq.it

***Abstract*— The successful deployment of Impulse Radio (IR) Ultra Wide Band (UWB) wireless communication systems requires that they coexist and contend with a variety of interfering signals co–located over the same transmission band. In fact, if on the one hand the large transmission bandwidth of IR–UWB signals allows them to resolve multipath components and exploit multipath diversity, on the other hand it yields some new coexistence challenges for both unlicensed commercial and military communication systems, which are required to be robust to unintentional and intentional jammers, respectively. In particular, the design and analysis of low–complexity receiver schemes with good synchronization capabilities and high robustness to Narrow–Band Interference (NBI) is acknowledged as an important issue in IR–UWB research. Motivated by this consideration, in [1] we have recently proposed a low–complexity receiver design, the so–called Chip–Time Differential Transmitted–Reference ($\mathrm{T_c}$–DTR) scheme, and have shown that it is more robust to NBI than other non–coherent receiver schemes available in the literature. In this paper, we aim at generalizing the results in [1] and at developing the enabling analytical tools for the analysis and design of timing acquisition algorithms for non–coherent receivers over frequency–selective fading channels with NBI. Furthermore, we move from the proposed analytical framework to tackle the optimization problem of devising optimal signature codes to reduce the impact of NBI on the performance of the $\mathrm{T_c}$–DTR synchronizer. Analytical frameworks and findings are substantiated via Monte Carlo simulations.**

I. Introduction

In Ultra Wide Band (UWB) research, the design of low–complexity receiver architectures has been receiving a continuously growing interest due to the inherent architectural complexity and non–negligible power consumptions required by optimal transceiver designs based on Rake combining and high speed time–interleaved Analog–to–Digital–Converters (ADCs). In fact, low–complexity, low–cost, and power–efficient UWB receiver schemes, which integrate communication, ranging/localization, and radar capabilities are envisaged to play a fundamental role in several emerging application areas for both unlicensed commercial and military wireless communication systems [2]. A good overview of history and applications of UWB technology can be found in [3], and a comprehensive survey and analysis of low–complexity (*i.e.*, non–coherent) receiver schemes is available in [4]. Also, the interested reader may consult the Special Issue on *Ultra–Wide Bandwidth (UWB) Technology & Emerging Applications* published in the Proceedings of the IEEE in February 2009 for the latest developments on UWB research.

Among the many low–complexity solutions for Impulse Radio (IR–) UWB wireless systems, the family of Transmitted–Reference (TR) signaling schemes has attracted, since its inception for UWB applications in 2002 [5], the interest of several researchers due to the inherent capability of these solutions of transmitting and receiving data over unknown fading channels. Since then, several non–coherent receiver schemes have been proposed in the open technical literature, such as the Energy Detector (ED) [6], the "dirty template" detector [7], the hybrid auto–correlation receiver [8], the Slightly Frequency–Shifted Reference (FSR) receiver [9], the Chip–Time Differential Transmitted–Reference ($\mathrm{T_c}$–DTR) scheme [10], the pulse cluster transmission system [11], and the Code–Multiplexed Transmitted–Reference scheme [12]. An up–to–date overview and comparison of these receivers is available in [13], [14], and, more recently, in [1] where a general scenario with multi–tone interference is considered.

In spite of the large body of literature on the design and performance evaluation of non–coherent receiver schemes over frequency–selective fading channels, the research contributions aiming at studying, designing, and optimizing the performance of these systems in the presence of NBI is quite limited. Some notable contributions are [15]–[21] and references therein. The interested reader might find in [13] and [14] a careful survey and comparison of recent literature. Furthermore, most of the above–mentioned literature is mainly concerned with data detection performance, while literature on timing acquisition performance in the presence of NBI is definitely insufficient because useful only in part for computing relevant performance metrics [10], [13], [14], [20]. However, the impact of non–system interference on the performance of UWB receivers, and, due to the incoherent processing, especially non–coherent schemes, is a very important research area, which if not adequately addressed might greatly limit the

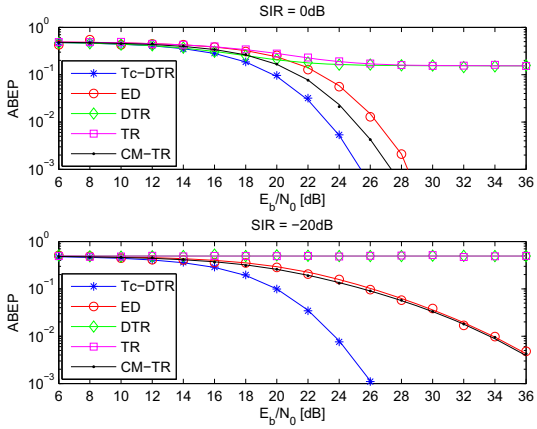

Fig. 1. ABEP against the Bit–Energy–to–Noise–Spectral–Density–Ratio ($\mathrm{E_b/N_0}$) and the Signal–to–Interference–Ratio (SIR). Legend: TR = Transmitted–Reference [16], DTR = Differential Transmitted–Reference [16], ED = Energy Detector [18], CM–TR = Coded–Multiplexed Transmitted–Reference [12], $\mathrm{T_c}$–DTR = Chip–Time Differential Transmitted–Reference [10]. A setup similar to [13, Fig. 1 and Fig. 2] is considered.

application scope of UWB technology because of its inherent underlay transmission mechanism [21]. This is especially true in military scenarios, where low–complexity timing acquisition solutions operating at low Signal–to–Noise–Ratio (SNR) over frequency–selective fading channels and intentional jamming play a crucial role [2].

Motivated by these considerations, in this paper we build upon and generalize our recent research studies on timing–acquisition for non–coherent receiver schemes over frequency–selective fading channels with NBI [14]. In particular, we consider the $\mathrm{T_c}$–DTR receiver scheme and develop an accurate framework for computing the Detection ($\mathrm{P_d}$) and False Alarm ($\mathrm{P_{fa}}$) Probability at any arbitrary time–lag, which are the fundamental performance metrics for understanding the synchronization capabilities of any receiver scheme and for estimating more general end–to–end performance metrics, such as the Mean Acquisition Time (MAT) and the Overall Acquisition Probability ($\mathrm{P_{d_{ov}}}$) [10]. Furthermore, we move from the proposed analytical framework to conceive the optimal code design that minimizes the impact of NBI on the performance of the $\mathrm{T_c}$–DTR receiver scheme.

More specifically, the rationale for considering the $\mathrm{T_c}$–DTR receiver in our study originates from [13], [14], where we have shown that our proposed solution outperforms any other non–coherent receiver scheme available in the literature. As an example, in Fig. 1 we show the Average Bit Error Probability (ABEP) of several well–known non–coherent receivers over a frequency–selective fading channel with a single–tone jammer. By exploiting the optimal code design in [13], the robustness to NBI of our receiver is apparent. Furthermore, the original contribution with respect to our past research is significant: in [1] and [14], $\mathrm{P_d}$ and $\mathrm{P_{fa}}$ are computed only at *zero time–lag*, which makes them useless for computing MAT and $\mathrm{P_{d_{ov}}}$, which, on the other hand, are the fundamental performance metrics for timing acquisition analysis, and require the knowledge of $\mathrm{P_d}$ and $\mathrm{P_{fa}}$ at *any time–lag* to be computed [10].

The remainder of this paper is organized as follows. In Section II, the system model and the $\mathrm{T_c}$–DTR receiver scheme are introduced. In Section III, the framework for computing $\mathrm{P_d}$ and $\mathrm{P_{fa}}$ at any time–lag in the presence of multipath and a faded single–tone jammer is described. In Section IV, we provide some guidelines to design the optimal code for NBI suppression with and without synchronization constraints. In Section V, the analytical framework is validated via Monte Carlo simulation and some results are shown. Finally, Section VI concludes the paper.

II. System Model

We consider the $\mathrm{T_c}$–DTR receiver scheme in [10, Fig. 1]. The aim of this section is to summarize the main elements of the system model useful for the derivation of the analytical framework in Section III.

A. Transmitted Signal

Let us consider a data–aided timing acquisition scheme [10], where the transmitted signal is given by an unmodulated train of short pulses:

$$s(t) = \sum_{j=-\infty}^{+\infty} \sqrt{E_w}\tilde{c}_j w(t - jT_c) \tag{1}$$

where $\{c_j\}_{j=0}^{N_s-1} \in \{-1,+1\}$ is the Direct Sequence (DS) signature code with period (*i.e.*, length) N_s, *i.e.*, $\{c_j\}_{j=0}^{N_s-1} = \{c_{j+N_s}\}_{j=0}^{N_s-1}$, and $\tilde{c}_j = c_j\tilde{c}_{j-1}$ is the differentially–encoded version of c_j. Moreover, T_c denotes the average pulse repetition period, *i.e.*, the chip time, $w(\cdot)$ is the band–pass transmitted pulse with duration $0 \leq T_w \leq T_c$, center frequency f_c, and unit energy (*i.e.*, $\int_0^{T_w} w^2(t)\,dt = 1$), $E_w = E_{\mathrm{cod}}/N_s$ and E_{cod} are pulse and codeword energies, respectively.

B. Channel Model

We consider a frequency–selective multipath fading propagation channel with single–tone interference. Accordingly, the received signal, $r(\cdot)$, can be written as follows:

$$r(t) = (s \otimes h)(t) + J(t) + n(t) \tag{2}$$

where $J(\cdot)$ is the jammer, $h(\cdot)$ is the channel impulse response, $\otimes$ denotes the convolution operator, and $n(\cdot)$ is the zero–mean Additive White Gaussian Noise (AWGN) with two–sided power spectral density $N_0/2$.

The impulse response, $h(\cdot)$, of a UWB channel is [22]:

$$h(t) = \sum_{l=0}^{L-1} \alpha_l \delta(t - \tau_l) \tag{3}$$

where α_l and τ_l are gain and delay of the l–path, respectively, and L is the number of received multipath components. Moreover, $\alpha_l = \beta_l p_l$, where β_l denotes the fading gain and p_l is a pulse polarity factor that takes values ± 1 with equal probability [22]. For analytical tractability, we consider the resolvable multipath channel assumption, *i.e.*, $|\tau_l - \tau_m| \geq T_w$, $\forall l \neq m$, where $\{\tau_l\}_{l=1}^{L-1} = \tau_0 + lT_w$. Moreover, to avoid Inter–Symbol (ISI) and Inter–Chip Interference (ICI), we consider $T_c \geq T_d$, where T_d denotes the maximum excess delay of the channel. Without loss of generality, we also assume $\tau_0 = 0$.

Similar to [13]–[16], [18], in typical UWB systems the NBI can be reasonably modeled as a tone interference, as follows:

$$J(t) = \sqrt{2J_0}\alpha_{J_0}\cos\left(2\pi f_{J_0}t + \theta_{J_0}\right) \tag{4}$$

$$\begin{cases} \mathrm{P_d}\left(\hat{\tau};\mathrm{D_{th}}|\left\{\alpha_l\right\}_{l=1}^{L_{\mathrm{cap}}},\alpha_{J_0}\right)=Q\left(\left.\dfrac{\mathrm{D_{th}}-\mu_{D_i}\left(\hat{\tau}|\left\{\alpha_l\right\}_{l=1}^{L_{\mathrm{cap}}},\alpha_{J_0}\right)}{\sigma^2_{D_i}\left(\hat{\tau}|\left\{\alpha_l\right\}_{l=1}^{L_{\mathrm{cap}}},\alpha_{J_0}\right)}\right|\hat{\tau}\in\mathscr{H}_1\right)=Q\left(\left.\dfrac{\mathrm{D_{th}}-\left[U_i\left(\hat{\tau}\right)+I_i\left(\hat{\tau}\right)\right]}{\mathrm{E}_n\left\{N_i^2\left(\hat{\tau}\right)\right\}}\right|\hat{\tau}\in\mathscr{H}_1\right) \\ \mathrm{P_{fa}}\left(\hat{\tau};\mathrm{D_{th}}|\left\{\alpha_l\right\}_{l=1}^{L_{\mathrm{cap}}},\alpha_{J_0}\right)=Q\left(\left.\dfrac{\mathrm{D_{th}}-\mu_{D_i}\left(\hat{\tau}|\left\{\alpha_l\right\}_{l=1}^{L_{\mathrm{cap}}},\alpha_{J_0}\right)}{\sigma^2_{D_i}\left(\hat{\tau}|\left\{\alpha_l\right\}_{l=1}^{L_{\mathrm{cap}}},\alpha_{J_0}\right)}\right|\hat{\tau}\in\mathscr{H}_0\right)=Q\left(\left.\dfrac{\mathrm{D_{th}}-\left[U_i\left(\hat{\tau}\right)+I_i\left(\hat{\tau}\right)\right]}{\mathrm{E}_n\left\{N_i^2\left(\hat{\tau}\right)\right\}}\right|\hat{\tau}\in\mathscr{H}_0\right) \end{cases} \tag{8}$$

where J_0, α_{J_0}, f_{J_0}, and θ_{J_0} are average received power, channel gain, carrier frequency, and phase of the interfering signal, respectively. Also, we assume a flat–fading and slowly–varying multipath channel model for the single–tone NBI.

C. Receiver Operations

The $\mathrm{T_c}$–DTR receiver works as follows [10]. First, the received signal, $r\left(\cdot\right)$, in (2) is passed through an ideal band–pass filter with bandwidth W and center frequency f_c to eliminate out–of–band noise and interference. Then, the signal, $\tilde{r}\left(t\right)=\left(s\otimes h\right)\left(t\right)+J\left(t\right)+\tilde{n}\left(t\right)$, at the filter output is multiplied by a T_c–delayed version of itself and weighted by a locally–generated gating waveform, $z\left(\cdot;\cdot\right)$, as follows:

$$z\left(t;\hat{\tau}\right)=\sum_{j=0}^{N_s-1}c_j g\left(t-jT_c-\hat{\tau}\right) \tag{5}$$

where[1] $\tilde{n}\left(\cdot\right)$ is the filtered Gaussian noise having auto–correlation function $R_{\tilde{n}}\left(\xi\right)=WN_0\mathrm{sinc}\left(\mathrm{W}\xi\right)\cos\left(2\pi f_c\xi\right)$, $g\left(t\right)=\mathrm{rect}\left(t/T_I-0.5\right)$, $0<T_I\leqslant T_c$ is the integration window, and $0\leq\hat{\tau}<N_sT_c$ is the trial time delay between received signal and local gating waveform, *i.e.*, the delay the timing synchronization unit needs to estimate according to a given performance criterion [10].

D. Timing Acquisition

Let us consider, for ease of illustration, a serial search synchronization method [23] and a threshold–based synchronizer [24]. Accordingly, the synchronization unit computes, for each trial time–shift $\hat{\tau}$, the correlation function [10, Fig. 1]:

$$D_i(\hat{\tau})=\int_{\hat{\tau}+iN_sT_c}^{\hat{\tau}+(i+1)N_sT_c}\tilde{r}\left(t\right)\tilde{r}\left(t-T_c\right)z\left(t-iN_sT_c;\hat{\tau}\right)dt \tag{6}$$

where $t\in\left[\hat{\tau}+iN_sT_c,\hat{\tau}+\left(i+1\right)N_sT_c\right)$ is the i–th observation window for signal detection.

Then, it uses the following decision logic:

1) If $D_i(\cdot)$ exceeds a given decision threshold $\mathrm{D_{th}}$, then the corresponding trial time–shift $\hat{\tau}$ is tentatively declared to be an in–phase cell ($\mathscr{H}_1$ cell[2]) and a verification stage is activated to confirm or dismiss the test. If the test is confirmed, the search is terminated and the detection phase can take place; otherwise the system resumes the time synchronization phase and another trial $\hat{\tau}$ is tested.
2) If $D_i(\cdot)$ does not exceed $\mathrm{D_{th}}$, the cell is declared to be an out–of–phase cell ($\mathscr{H}_0$ cell) and a next cell, selected according to a given search logic [23], is tested.

Thus, the performance of the decision logic is subject, for each $\hat{\tau}$, to undesired events, which depend on the presence of noise, interference, and multipath fading. More specifically, a *False Alarm* occurs when the integrator output exceeds the threshold for a $\mathscr{H}_0$ cell, and a *Miss* (*Detection*) occurs when the integrator output is below (above) the threshold for a $\mathscr{H}_1$ cell. Therefore, the performance of a threshold–crossing synchronizer can be completely described in terms of Detection ($\mathrm{P_d}\left(\cdot,\cdot\right)$) and False Alarm ($\mathrm{P_{fa}}\left(\cdot,\cdot\right)$) probabilities[3]:

$$\begin{cases} \mathrm{P_d}\left(\hat{\tau};\mathrm{D_{th}}\right)=\Pr\left\{D_i\left(\hat{\tau}\right)>\mathrm{D_{th}}|\,\hat{\tau}\in\mathscr{H}_1\right\} \\ \mathrm{P_{fa}}\left(\hat{\tau};\mathrm{D_{th}}\right)=\Pr\left\{D_i\left(\hat{\tau}\right)>\mathrm{D_{th}}|\,\hat{\tau}\in\mathscr{H}_0\right\} \end{cases} \tag{7}$$

where $\Pr\left\{\cdot\right\}$ means probability.

The functions defined in (7) represent the fundamental metrics needed to study the end–to–end timing acquisition performance (*i.e.*, MAT and $\mathrm{P_{d_{ov}}}$) of any receiver, and, in particular, the $\mathrm{T_c}$–DTR scheme [10].

III. Analytical Framework: $\mathrm{P_d}$ and $\mathrm{P_{fa}}$

To develop a simple and insightful analytical model, we retain two main assumptions. 1) Similar to [14], we exploit the Gaussian approximation for the cross–noise term in (6), which arises from TR operations. We emphasize that no Gaussian approximation is considered to analytically modeling the single–tone NBI. 2) For analytical simplicity, we assume that the uncertainty region $[0,N_sT_c)$ is quantized into a finite number of cells, through which the gating waveform is shifted in steps of a unit search interval T_w, *i.e.*, the pulse width. Accordingly, we define $\hat{\tau}=\hat{\mu}_cT_c+\hat{\mu}_wT_w$ with $\hat{\mu}_c=\lfloor\hat{\tau}/T_c\rfloor\in\left\{0,1,\ldots,N_s-1\right\}$ and $\hat{\mu}_w=\left(\hat{\tau}-\hat{\mu}_cT_c\right)/T_w\in\left\{0,1,\ldots,N_w-1\right\}$, where $\lfloor\cdot\rfloor$ is the floor function and $N_w=T_c/T_w$ is a positive integer number.

After some algebraic manipulations, $\mathrm{P_d}$ and $\mathrm{P_{fa}}$ can be written as shown in (8) on top of this page, where:

- We have emphasized that $\mathrm{P_d}$ and $\mathrm{P_{fa}}$ depend on the fading channel statistics of the useful (UWB) user and the single–tone jammer;
- L_{cap} is the number of captured multipath components within the integration window T_I, which is defined as $L_{\mathrm{cap}}=\lfloor T_I/T_w\rfloor$ with $0\leq L_{\mathrm{cap}}\leq L$;
- $\mathrm{E}_n\left\{\cdot\right\}$ is the expectation computed over the AWGN;
- $Q\left(x\right)=\left(1/\sqrt{2\pi}\right)\int_x^{+\infty}\exp\left(-t^2/2dt\right)$;
- $\mu_{D_i}\left(\cdot|\cdot,\cdot\right)$ and $\sigma_{D_i}\left(\cdot|\cdot,\cdot\right)$ are the mean and standard deviation of Random Variable (RV) $D_i\left(\cdot\right)$ in (6) computed over the AWGN, *i.e.*, $\mu_{D_i}\left(\hat{\tau}|\left\{\alpha_l\right\}_{l=1}^{L_{\mathrm{cap}}},\alpha_{J_0}\right)=\mathrm{E}_n\left\{D_i\left(\hat{\tau}\right)\right\}=U_i\left(\hat{\tau}\right)+I_i\left(\hat{\tau}\right)$ and $\sigma^2_{D_i}\left(\hat{\tau}|\left\{\alpha_l\right\}_{l=1}^{L_{\mathrm{cap}}},\alpha_{J_0}\right)=\mathrm{E}_n\left\{\left[D_i\left(\hat{\tau}\right)-\mathrm{E}_n\left\{D_i\left(\hat{\tau}\right)\right\}\right]^2\right\}=\mathrm{E}_n\left\{N_i^2\left(\hat{\tau}\right)\right\}$, respectively. With this notation, we have assumed that

[1] $\mathrm{rect}\left(t/2T\right)=1$ if $-T\leq t\leq T$ and $\mathrm{rect}\left(t/2T\right)=0$ elsewhere; and $\mathrm{sinc}\left(x\right)=\sin\left(x\right)/x$ if $x\neq0$ and $\mathrm{sinc}\left(0\right)=1$.

[2] In–phase, $\mathscr{H}_1$, and out–of–phase cells, $\mathscr{H}_0$, are identified according to the given performance criterion of interest [10].

[3] In the notation we have emphasized that $\mathrm{P_d}$ and $\mathrm{P_{fa}}$ depend on the trial time shift $\hat{\tau}$ and the synchronization threshold $\mathrm{D_{th}}$.

$$\sigma^2_{D_i}\left(\hat{\tau}|\left\{\alpha_l\right\}_{l=1}^{L_{\rm cap}},\alpha_{J_0}\right)=\mathrm{E}_n\left\{N_i^2\left(\hat{\tau}\right)\right\}\cong N_sE_wN_0\left(\sum_{l=\hat{\mu}_w}^{\min\left\{L_{\rm cap}+\hat{\mu}_w-1,N_w-1\right\}}\beta_l^2+\sum_{l=0}^{\max\left\{L_{\rm cap}+\hat{\mu}_w-1-N_w,0\right\}}\beta_l^2\right)$$
$$+N_0E_w\left(\sum_{j=0}^{N_s-1}c_jc_{j-1}\tilde{c}_{j+\hat{\mu}_c}\tilde{c}_{j+\hat{\mu}_c-2}\right)\left(\sum_{l=\hat{\mu}_w}^{\min\left\{L_{\rm cap}+\hat{\mu}_w-1,N_w-1\right\}}\beta_l^2\right)$$
$$+N_0E_w\left(\sum_{j=0}^{N_s-1}c_jc_{j-1}\tilde{c}_{j+\hat{\mu}_c+1}\tilde{c}_{j+\hat{\mu}_c-1}\right)\left(\sum_{l=0}^{\max\left\{L_{\rm cap}+\hat{\mu}_w-1-N_w,0\right\}}\beta_l^2\right) \tag{11}$$
$$+N_sN_0T_IJ_0\alpha_{J_0}^2+N_0T_IJ_0\alpha_{J_0}^2\cos\left(4\pi f_{J_0}T_c\right)\sum_{j=0}^{N_s-1}c_jc_{j-1}+\frac{N_sN_0^2WT_I}{2}$$

$D_i\left(\cdot\right)$ in (6) can be decomposed into the summation of three contributions $U_i\left(\cdot\right)$, $I_i\left(\cdot\right)$, and $N_i\left(\cdot\right)$, which are useful, interference, and noise terms, respectively.

According to [10], either the conditional $\mathrm{P_d}$ and $\mathrm{P_{fa}}$ in (8) or the average (over the channel gains) $\mathrm{P_d}$ and $\mathrm{P_{fa}}$, *i.e.*[4], $\mathrm{P_d}\left(\hat{\tau};\mathrm{D_{th}}\right)=\mathrm{E}_{\left\{\alpha_l\right\}_{l=1}^{L_{\rm cap}},\alpha_{J_0}}\left\{\mathrm{P_d}\left(\hat{\tau};\mathrm{D_{th}}|\left\{\alpha_l\right\}_{l=1}^{L_{\rm cap}},\alpha_{J_0}\right)\right\}$, $\mathrm{P_{fa}}\left(\hat{\tau};\mathrm{D_{th}}\right)=\mathrm{E}_{\left\{\alpha_l\right\}_{l=1}^{L_{\rm cap}},\alpha_{J_0}}\left\{\mathrm{P_{fa}}\left(\hat{\tau};\mathrm{D_{th}}|\left\{\alpha_l\right\}_{l=1}^{L_{\rm cap}},\alpha_{J_0}\right)\right\}$, might be needed to compute MAT and $\mathrm{P_{d_{ov}}}$: this depends on the assumption of slowly– or fast–fading varying channel conditions, respectively.

In summary, from the analysis above it follows that $\mathrm{P_d}$ and $\mathrm{P_{fa}}$ can be computed if accurate expressions of $U_i\left(\cdot\right)$, $I_i\left(\cdot\right)$, and $\mathrm{E}_n\left\{N_i^2\left(\cdot\right)\right\}$ can be obtained at any time–lag $\hat{\tau}$.

A. Closed–Form Computation of $U_i\left(\cdot\right)$, $I_i\left(\cdot\right)$, $\mathrm{E}_n\left\{N_i^2\left(\cdot\right)\right\}$

From (6), and after some lengthly algebraic manipulations, $U_i\left(\cdot\right)$ and $I_i\left(\cdot\right)$ can be written as follows:

$$U_i\left(\hat{\tau}\right)=\left(\sum_{j=0}^{N_s-1}c_jc_{j+\hat{\mu}_c}\right)\left(\sum_{l=\hat{\mu}_w}^{\min\left\{L_{\rm cap}+\hat{\mu}_w-1,N_w-1\right\}}\beta_l^2\right)E_w$$
$$+\left(\sum_{j=0}^{N_s-1}c_jc_{j+\hat{\mu}_c+1}\right)\left(\sum_{l=0}^{\max\left\{L_{\rm cap}+\hat{\mu}_w-1-N_w,0\right\}}\beta_l^2\right)E_w \tag{9}$$

$$I_i\left(\hat{\tau}\right)\cong J_0T_I\alpha_{J_0}^2\cos\left(2\pi f_{J_0}T_c\right)\sum_{j=0}^{N_s-1}c_j \tag{10}$$

where $\min\left(\cdot,\cdot\right)$ and $\max\left(\cdot,\cdot\right)$ are the minimum and maximum functions, respectively; and in (10) we have taken into account that, for typical system setups, we have $T_I\gg\left(4\pi f_{J_0}\right)^{-1}$.

Furthermore, by exploiting some properties of multi–variate Gaussian processes, the noise variance, $\mathrm{E}_n\left\{N_i^2\left(\cdot\right)\right\}$, in (8) can be computed as shown in (11) on top of this page. We notice that there are several terms in (11), especially those related to the NBI, which are independent of the time–shift $\hat{\tau}$. In Section IV, we will see that this result greatly simplifies the design of the optimal code to reduce the impact of NBI.

IV. Optimal Code Design

From the analytical model in Section III, we can obtain the optimal code design to almost completely reducing to zero the impact of the single–tone NBI. By direct inspection, the following objective functions for code design can be obtained:

$$\begin{cases}\mathrm{C}_1: & \cos\left(2\pi f_{J_0}T_c\right)\sum_{j=0}^{N_s-1}c_j=0\\ \mathrm{C}_2: & \cos\left(4\pi f_{J_0}T_c\right)\sum_{j=1}^{N_s-1}c_jc_{j-1}=-N_s\end{cases} \tag{12}$$

Very surprisingly, we can notice that (12) is exactly the same as [13, Eq. (16)], which is the optimal code design to minimizing the effect of NBI in the ABEP with perfect time synchronization at the receiver, and [14, Eq. (16)], which is the optimal code design to minimizing the effect of NBI in $\mathrm{P_d}$ and $\mathrm{P_{fa}}$ at zero time–lag. This is a very important, and a priori unpredictable, result: it tells us that with the code in (12) we can guarantee the same robustness to NBI for *each* time–shift between received signal and local template. In other words, from the point of view of the NBI, the optimization of the end–to–end timing acquisition performance metrics (MAT and $\mathrm{P_{d_{ov}}}$), which encompasses *all* the time–shifts $\hat{\tau}$, reduces to the optimization of $\mathrm{P_d}$ and $\mathrm{P_{fa}}$ at, *e.g.*, zero time–lag only. Furthermore, this optimality condition holds for other performance metrics, such as the ABEP. Since (12) is the same as in [13] and [14], we invite the interested reader to consult directly these two papers to obtain a detailed physical interpretation of (12) for code design.

A. Synchronization Constraints

The optimal code design in (12) allows us to reduce the impact of the NBI, however the resulting code is not necessarily a *good* code from the point of view of making robust the overall timing acquisition process [25]. In general, C_1 is a property the most DS codes almost satisfy, since most of known codes are well balanced. On the other hand, C_2 needs to be carefully investigated. C_2 imposes a constraint on the (partial) auto–correlation of the DS code evaluated at T_c. Often, both partial and cyclic auto–correlation functions of DS codes are chosen in order to have a very peaky main lobe in order to let the synchronization unit estimates more easily the zero time–lag (*e.g.*, for fine ranging purposes). On the contrary, if, for example, $\cos\left(4\pi f_{J_0}T_c\right)=-1$, then the optimal code design in (12) would require $\sum_{j=1}^{N_s-1}c_jc_{j-1}\cong N_s$, which, in practice[5], results in $\sum_{j=1}^{N_s-1}c_jc_{j-1}=N_s-1$. We observe that

[4] $\mathrm{E}_{\left\{\alpha_l\right\}_{l=1}^{L_{\rm cap}},\alpha_{J_0}}\left\{\cdot\right\}$ is the expectation computed over the channel fading.

[5] As mentioned in [14], C_2 can only be closely approximated.

the optimal code in (12) does not necessarily lead to a code with good synchronization capabilities from the point of view of ranging accuracy, since the correlation function has a very large main lobe spanning two chip times. A careful study of the optimal code design which, at the same time, can offer excellent robustness to NBI and excellent synchronization capabilities (according to either ranging or ABEP performance criteria [10]) is far beyond the scope of this paper and is currently being investigated. Additional constraints, such as spectral flatness and rejection to multiple–access interference, are also being taken into account in our research activity.

V. Numerical and Simulation Results

Due to space constraints, in this paper we do not show performance results related to MAT and $\mathrm{P_{d_{ov}}}$, but limit ourselves to analyze the average $\mathrm{P_d}\left(\hat{\tau};\mathrm{D_{th}}\right)$ and $\mathrm{P_{fa}}\left(\hat{\tau};\mathrm{D_{th}},\right)$ defined in Section III. The interested reader may obtain MAT and $\mathrm{P_{d_{ov}}}$ curves by simply substituting the framework proposed in this paper into the Markov chain model in [10].

The following system setup is considered for illustrative purposes: i) $T_w = 5\mathrm{ns}$, ii) $T_c = 60\mathrm{ns}$, iii) $N_s = 32$, iv) the channel is assumed to be dense and resolvable with $L = 10$, v) the multipath gains are Nakagami–*m* distributed with fading severity index $m = 2.5$, average power $\mathrm{E}\left\{\alpha_l^2\right\} = \mathrm{E}\left\{\alpha_0^2\right\}\exp\left(-\varepsilon l\right)$ for $l = 0, 1, \ldots, L-1$, and are normalized such that $\sum_{l=0}^{L-1}\mathrm{E}\left\{\alpha_l^2\right\} = 1$ with $\varepsilon = 0.45$, vi) $T_I = 20\mathrm{ns}$, which yields $L_{\mathrm{cap}} = 4$, vii) $f_{J_0} = 1\mathrm{GHz}$, which is approximately located around the peak of the pulse spectrum, viii) α_{J_0} is assumed to be Rayleigh distributed with $\mathrm{E}\left\{\alpha_{J_0}^2\right\} = 1$, ix) the decision threshold D_{th} is chosen according to a Constant False Alarm Rate (CFAR) optimization criterion [24] with $\mathrm{P_{fa}} = 10^{-3}$ at the corresponding time–lag $\hat{\tau}$ of interest, and x) the Signal–to–Interference–Ratio (SIR) is defined as $\mathrm{SIR} = (N_s E_w)/(J_0 N_s T_c)$.

To validate the optimal code design in (12) two DS codes are analyzed:

1) The first code, which is here called "Non–Optimal Code Design" does not satisfy both $\mathrm{C_1}$ and $\mathrm{C_2}$ in (12), but just $\mathrm{C_1}$ is satisfied while the cyclic auto–correlation of the code, *i.e.*, $\sum_{j=0}^{N_s-1} c_j c_{j-1}$, is equal to zero. This code design might correspond to a typical code used to get good synchronization capabilities for ranging purposes. The chosen code is Code1 = [1, -1, -1, -1, 1, 1, 1, -1, -1, -1, -1, -1, 1, -1, -1, 1, 1, 1, -1, 1, -1, -1, 1, -1, 1, -1, 1, 1, 1, -1, 1, 1].
2) The second code, which is here called "Optimal Code Design" satisfies both $\mathrm{C_1}$ and $\mathrm{C_2}$ in (12). The chosen code is Code2 = [-1, 1, -1, 1, -1, 1, -1, 1, -1, 1, -1, 1, -1, 1, -1, 1, -1, 1, -1, 1, -1, 1, -1, 1, -1, 1, -1, 1, -1, 1, -1, 1]. We observe an important property: it has a regular structure, which is known to not be a good choice for accurate ranging applications since it leads to a periodic auto–correlation function with high side–lobes. We have deliberately chosen this code in our example to provide a worst–case proof of the claim made in Section IV-A about the need to designing codes with both NBI rejection and timing acquisition capabilities for a global system–level optimization perspective.

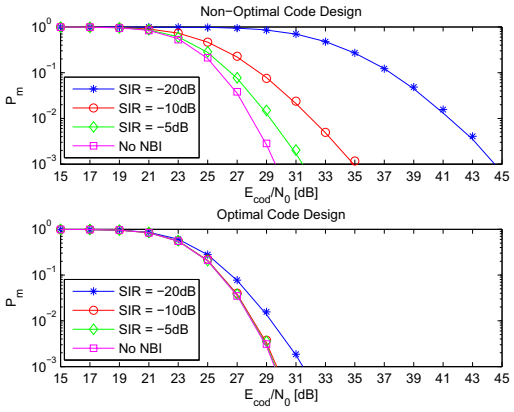

Fig. 2. Miss Probability ($\mathrm{P_m}$) against E_{cod}/N_0. Setup with $\hat{\mu}_c = 0$ and $\hat{\mu}_w = 0$. Markers: Monte Carlo simulation; solid lines: analytical model.

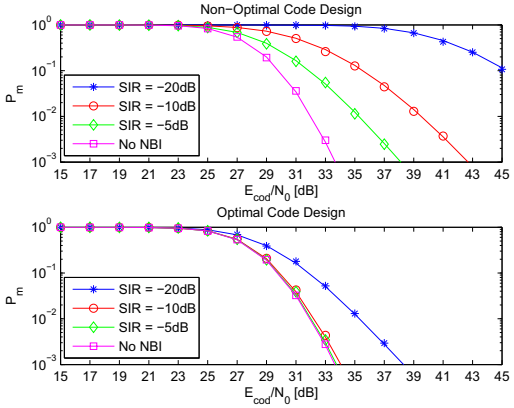

Fig. 3. Miss Probability ($\mathrm{P_m}$) against E_{cod}/N_0. Setup with $\hat{\mu}_c = 0$ and $\hat{\mu}_w = 2$. Markers: Monte Carlo simulation; solid lines: analytical model.

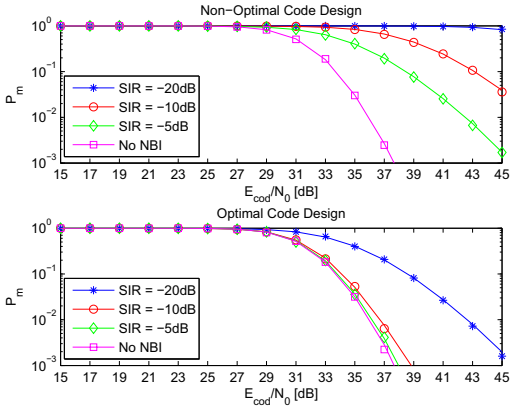

Fig. 4. Miss Probability ($\mathrm{P_m}$) against E_{cod}/N_0. Setup with $\hat{\mu}_c = 0$ and $\hat{\mu}_w = 4$. Markers: Monte Carlo simulation; solid lines: analytical model.

In Figs. 2–5, we show the Miss Probability, $\mathrm{P_m} = 1 - \mathrm{P_d}$, averaged over the fading channel statistics and obtained with both Monte Carlo simulations and the analytical model developed in Section III. Each figure shows a different value of the trial time–lag $\hat{\tau}$. In particular, Fig. 1 shows the achievable performance when the receiver if perfectly time–synchronized with the local template, *i.e.*, $\hat{\tau} = 0$. Overall, we can observe a very good match between Monte Carlo simulations and analytical model. Also, we observe that the "Optimal Code Design" according to (12) offers a significant performance gain with respect to the "Non–Optimal Code Design", and the gain increases with increasing values of the interfering

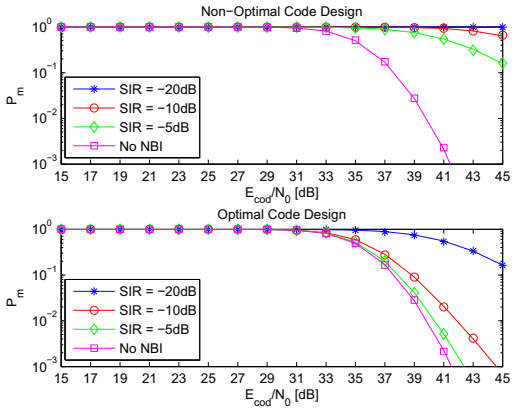

Fig. 5. Miss Probability ($\mathrm{P_m}$) against E_{cod}/N_0. Setup with $\hat{\mu}_c = 0$ and $\hat{\mu}_w = 6$. Markers: Monte Carlo simulation; solid lines: analytical model.

power. We note that the "Optimal Code Design" offers high robustness to NBI for low values of the SIR, with a negligible performance penalty, up to SIR = -10dB, with respect to the no NBI scenario. The reason why the code design in (12) does not allow a complete rejection of the NBI is due to C_2, which cannot be perfectly achieved. For example, with the setup used in this paper, Code2 gives $\cos\left(4\pi f_{J_0} T_c\right) \sum_{j=1}^{N_s-1} c_j c_{j-1} = 31 < N_s$ with $N_s = 32$. At very low SIRs (*e.g.*, SIR = -20dB in our setup) the power of the single–tone interferer is so high that even this small difference might be non–negligible.

Finally, by comparing Fig. 2 and Fig. 5 it seems that the code design in (12) does not offer the same robustness to NBI for each time–lag. In particular, it seems to be less robust for increasing values of $\hat{\tau}$: a result that would contradict the claim in Section III and according to which the code design in (12) should be independent of the actual time–lag $\hat{\tau}$. However, the reason for the apparently reduced robustness shown in Fig. 5 by Code2 is different, and is related to our definition of SIR. More specifically, for increasing values of $\hat{\tau}$ we need to take into account that the energy captured by the $\mathrm{T_c}$–DTR receiver is lower than that captured with perfect time alignment between received signal and gating waveform. This is due to the exponentially–decaying power–delay–profile of the channel model adopted in our simulations, and it is confirmed by (9), which is the useful collected energy at the detector input. On the other hand, the definition of the SIR adopted in this paper is related to the perfect time alignment condition. In other words, for increasing values of $\hat{\tau}$ the effective SIR seen by the receiver gets lower, thus resulting in a higher interfering power and a more pronounced effect on the system performance. This motivates the (apparently) less robustness of (12) for increasing values of $\hat{\tau}$. These results confirm the optimality of the code design in (12) for any $\hat{\tau}$.

VI. Conclusion

In this paper, we have proposed an accurate analytical framework for computing relevant performance metrics for timing acquisition analysis of the recently proposed $\mathrm{T_c}$–DTR receiver. Furthermore, the optimal code design for reducing the impact of NBI has been identified and it has been shown that the optimization condition is independent of the actual time asynchronism between received signal and local template. Ongoing research is now concerned with the derivation of the optimal code design in order to simultaneously satisfy good NBI rejection and fast/accurate timing acquisition capabilities.

References

[1] M. Di Renzo, D. De Leonardis, F. Graziosi, and F. Santucci, "$\mathrm{T_c}$–DTR: A low–complexity UWB receiver robust to narrow–band interference – Performance analysis and optimization", *IEEE Trans. Wireless Commun.*, Mar. 2010 (submitted, second round of revision).

[2] S. Colson and H. Hoff, "Ultra–wideband technology for defence applications", *IEEE Int. Conf. on Ultra–Wideband*, pp. 615–620, Sept. 2005.

[3] M. Z. Win, *et al.*, "History and applications of UWB", *Proc. of the IEEE*, vol. 97, no. 2, pp. 198–204, Feb. 2009.

[4] K. Witrisal, G. Leus, G. J. M. Janssen, M. Pausini, F. Troesch, T. Zasowski, and J. Romme, "Noncoherent ultra–wideband systems", *IEEE Sig. Process. Mag.*, vol. 26, no. 4, pp. 48–66, July 2009.

[5] R. Hoctor and H. Tomlinson, "Delay–hopped transmitted–reference RF communications", *IEEE UWBST*, pp. 265-269, May 2002.

[6] M. Weisenhorn and W. Hirt, "Robust non–coherent receiver exploiting UWB channel properties", *IEEE UWBST*, pp. 156–160, May 2004.

[7] L. Yang and G. B. Giannakis, "Timing ultra–wideband signals with dirty templates", *IEEE Trans. Commun.*, vol. 53, pp. 1952–1963, Nov. 2005.

[8] F. Tufvesson, S. Gezici, and A F. Molisch, "Ultra–wideband communications using hybrid matched filter correlation receivers", *IEEE Trans. Wireless Commun.*, vol. 5, no. 11, pp. 3119–3129, Nov. 2006.

[9] D. Goeckel and Q. Zhang, "Slightly frequency–shifted reference ultra–wideband radio", *IEEE Trans. Commun.*, vol. 55, pp. 508–519, 2007.

[10] M. Di Renzo, L. A. Annoni, F. Graziosi, and F. Santucci, "A novel class of algorithms for timing acquisition of differential transmitted reference UWB receivers: Architecture, performance analysis and system design", *IEEE Trans. Wireless Commun.*, vol. 7, no. 6, pp. 2368–2387, June 2008.

[11] X. Dong, L. Jin, and P. Orlik, "A new transmitted reference pulse cluster system for UWB communications", *IEEE Trans. Vehic. Technol.*, vol. 57, no. 5, pp. 3217–3224, Sept. 2008.

[12] A. D'Amico, U. Mengali, "Code–multiplexed UWB transmitted–reference radio", *IEEE Trans. Commun.*, vol. 56, pp. 2125–2132, 2008.

[13] M. Di Renzo, D. De Leonardis, F. Graziosi, and F. Santucci, "On the robustness of $\mathrm{T_c}$–DTR UWB receivers to narrow–band interference: Performance analysis and guidelines for system optimization", *IEEE ICUWB*, pp. 77–82, Sept. 2009.

[14] M. Di Renzo, D. De Leonardis, F. Graziosi, and F. Santucci, "Detection and false alarm probabilities of IR–UWB Chip–Time Differential Transmitted–Reference receivers: A framework for performance analysis and optimization over multipath fading channels with tone interference", *IEEE MILCOM*, pp. 1–9, Oct. 2009.

[15] A. Giorgetti, M. Chiani, and M. Z. Win, "The effect of narrowband interference on wideband wireless communication systems", *IEEE Trans. Commun.*, vol. 53, no. 12, pp. 2139–2149, Dec. 2005.

[16] T. Quek, M. Z. Win, D. Dardari, "Unified analysis of UWB transmitted–reference schemes in the presence of narrowband interference", *IEEE Trans. Wireless Commun.*, vol. 6, pp. 2126–2139, June 2007.

[17] Y. D. Alemseged and K. Witrisal, "Modeling and mitigation of narrowband interference for transmitted–reference UWB systems", *IEEE J. Select. Signal Process.*, vol. 1, no. 3, pp. 456–469, Oct. 2007.

[18] A. Rabbachin, "Low complexity UWB receivers with ranging capabilities", *Ph.D. Dissertation*, University of Oulu, May 2008.

[19] M. Chiani and A. Giorgetti, "Coexistence between UWB and narrow–band wireless communication systems", *Proc. of the IEEE*, vol. 97, no. 2, pp. 231–254, Feb. 2009.

[20] M. Di Renzo, F. Graziosi, and F. Santucci, "On the cumulative distribution function of quadratic–form receivers over generalized fading channels with tone interference", *IEEE Trans. Commun.*, vol. 57, no. 7, pp. 2122–2137, July 2009.

[21] P. C. Pinto, A. Giorgetti, M. Z. Win, and M. Chiani, "A stochastic geometry approach to coexistence in heterogeneous wireless networks", *IEEE J. Sel. Areas Commun.*, vol. 27, no. 7, pp. 1268–1282, Sept. 2009.

[22] A. F. Molisch, "Ultrawideband propagation channels – Theory, measurement, and modeling", *IEEE Trans. Veh. Technol.*, vol. 54, no. 5, pp. 1528–1545, Sept. 2005.

[23] A. Polydoros and C. Weber, "A unified approach to serial search spread spectrum code acquisition: Part I. General theory", *IEEE Trans. Commun.*, vol. 32, no. 5, pp. 542-549, May 1984.

[24] J. H. J. Iinatti, "On the threshold setting principles in code acquisition of DS–SS signals", *IEEE J. Sel. Areas Commun.*, vol. 18, no. 1, pp. 62-72, Jan. 2000.

[25] S. W. Golomb and G. Gong, *Signal Design for Good Correlation: For Wireless Communication, Cryptography, and Radar*, Cambridge University Press, July 2005.